Atomic-binding effects in inelastic νe scattering

A. B. Dobrotsvetov, S. A. Fayans, and V. Yu. Dobretsov
I. V. Kurchatov Institute of Atomic Energy, 123182, Moscow

(Submitted 21 February 1992)
Pis'ma Zh. Eksp. Teor. Fiz. **55**, No. 9, 483–489 (10 May 1992)

The energy spectra of the electrons knocked out of various atomic shells in the course of νe scattering are calculated in the minimal electroweak model. The electromagnetic form factors of the neutrino are taken into account. These spectra are found to be quite different from those in the case of free scattering. These differences are found not only when the energies of the impinging neutrinos are comparable to the binding energy of the electron but also at energies an order of magnitude greater. For a scattering due to the magnetic moment, the cross section for bound electrons is always smaller than that for free electrons. The spectrum of recoil electrons does not diverge at small kinetic energies. It cuts off in a natural way and has a plateau. The role played by these effects in the scattering of fission-reactor $\tilde{\nu}_e$'s is examined.

The scattering of neutrinos by electrons is a fundamental process, and research on it is of particular importance. This scattering is the sole case of a purely leptonic weak process which can be studied in the laboratory, with the help of either neutrino sources on the earth (β-decaying nuclei, reactors, and accelerators) or sources in space (the sun, supernovae, etc.). At present, all the experimental data available on νe scattering, for both muon neutrinos and electron neutrinos, agree with the predictions of the Weinberg–Salam–Glashow minimal electroweak model. Although the experimental data presently available are not highly accurate in all cases, the brilliant success of this model is undeniable. Experimentalists and theoreticians have turned their efforts to seeking effects which lie outside the standard model. Foremost among these effects are processes which might result from such hypothetical properties of neutrinos as a non-vanishing mass and/or anomalously large electromagnetic form factors. These properties could lead to spin flip and oscillations of neutrinos, rendering them undetectable (in the weak-interaction channel). Interest in such effects has arisen primarily because of two factors, the first being the so-called solar-neutrino paradox: The count rate of neutrino events in the experiment of Ref. 1 was too low (i.e., lower by a factor of about 3 than that predicted by the standard solar model). Second, there are indications of an anticorrelation between this count rate and the level of solar activity.[2] The most attractive explanation is a combination of a resonant amplification of neutrino oscillations in solar matter[3,4] with a spin and spin-flavor precession[5,6] in magnetic fields. Here the neutrino would have to have, at the very least, a magnetic moment which is not very small. Experiments[7,8] on the scattering of reactor $\tilde{\nu}_e$'s impose the limitation[9,10] $\mu_{\tilde{\nu}_e} < 3\times 10^{-10}\mu_B$ [but see Ref. 11, where a more accurate spectrum of reactor $\tilde{\nu}_e$'s led to the value $\mu_{\tilde{\nu}_e} = (2\text{–}4)\times 10^{-10}\mu_B$ for the experiment of Ref. 7]. The limitation on the magnetic moment of the electron neutrino which was found at LAMPF is an order of magnitude worse.[12] Analysis of astrophysical data on red giants has yielded the more severe limitation[13] $\mu_{\bar{\nu}} < 3 \times 10^{-12} \mu_B$. Even under this severe limitation, however, the solar data can be explained by the mechanism of spin-flavor precession.[6]

Consequently, it is a matter of great interest to measure $\mu_{\bar{\nu}}$ or to find even more severe limitations on it. The only appropriate process for such studies is νe scattering. The reason is that one could hope to observe such small values of $\mu_{\bar{\nu}}$ only in situations in which the magnetic-scattering component of the total cross section is a measurable fraction of the electroweak cross section. The latter increases with increasing neutrino energy. The magnetic-scattering cross section, in contrast, diverges logarithmically at the lower limit of the spectrum of the detected recoil particle, as can be seen in the example of free νe scattering.[11] One could thus hope for success by detecting recoil electrons with a small kinetic energy. Although such experiments are very difficult, because the effect is small, and the background conditions are bad, technological developments in experimental physics may eventually make such measurements feasible (Ref. 14, for example). At that point, of course, effects of the electron binding in atoms must be taken into account appropriately.

In the present letter we examine inelastic low-energy νe scattering by atomic electrons in a process accompanied by ionization of the atom. In this case we have the following expressions for the matrix elements of the process:

$$M_{fi}^{(w)} = -\frac{G_F}{\sqrt{2}\hbar c}\bar{u}_{\vec{p}\lambda_{\nu_2}}\gamma^\mu(1+\gamma^5)u_{\vec{p}\lambda_{\nu_1}}$$

$$\times \int d^3r \bar{\psi}^{(-)}_{\vec{p}\lambda_{e_2}}(\vec{r})\gamma_\mu(g_V + g_A\gamma^5)\psi_{njlm_{e_1}}(\vec{r})e^{-i\vec{q}\vec{r}/\hbar}, \quad (1)$$

$$M_{fi}^{(\gamma)} = -\frac{4\pi e^2\hbar}{c}\bar{u}_{\vec{p}\lambda_{\nu_2}}\frac{\Gamma^\mu(q)}{(q^{(0)})^2 - (\vec{q})^2}u_{\vec{p}\lambda_{\nu_1}}\int d^3r\bar{\psi}^{(-)}_{\vec{p}\lambda_{e_2}}(\vec{r})\gamma_\mu\psi_{njlm_{e_1}}(\vec{r})e^{-i\vec{q}\vec{r}/\hbar}. \quad (2)$$

Here Γ^μ is the electromagnetic vertex, given by

$$\Gamma^\mu(q) = F_1(q)\gamma^\mu - \frac{F_2(q)}{2m_\nu c}\sigma^{\mu\nu}q_\nu, \quad (3)$$

where q is the 4-momentum transfer. At small values of q the electromagnetic form factors of the neutrino are

$$F_1(q) = \frac{1}{6}\frac{q^2}{\hbar^2} < r^2 >, \quad F_2(q) = \mu_\nu \frac{m_\nu}{m_e}, \quad (4)$$

where μ_ν is the magnetic moment of the neutrino, expressed in Bohr magnetons $\mu_B = e\hbar/2m_e c$. The quantity $u_{\vec{p}\lambda}$ in (1) and (2) is the amplitude of the ultrarelativistic impinging Dirac neutrino, with a momentum $\vec{p}$ and a helicity λ ($\lambda_{\nu_1} = -1$). In the standard model we would have $g_V = 1/2 + 2\sin^2\theta_W$ and $g_A = 1/2$ for the electron neutrino. The contribution of the charge radius of the neutrino can be transferred from

(1) to (2) by making the substitution $g_V \to g'_V = g_V + x$, where $x = \sqrt{2}\pi e^2 \langle r^2 \rangle / 3G_F$. The initial electron, e_1, is assumed to be in a bound state in an atomic subshell with principal quantum number n_1 and angular quantum numbers $j_1 l_1 m_1$. The final electron, e_2, is assumed to be in the continuous spectrum, with a polarization λ_2 and a momentum $\vec{p}_2$ at infinity. Its wave function is written as a partial-wave expansion. The differential cross section per atomic electron is expressed in terms of matrix elements (1) and (2) in the following way:

$$\frac{d\sigma}{dT_e}(T_e, E_{\nu_1}, njl_{e_1}) = \frac{p_{\nu_2} p_{e_2}}{2^8 \pi^5 \hbar^5 p_{\nu_1}(2j_1 + 1)} \times \sum_{m_1} \sum_{\lambda_{e_2}} \int do_{e_2} \sum_{\lambda_{\nu_2}} \int do_{\nu_2} |M_{fi}^{(\omega)} + M_{fi}^{(\gamma)}|^2, \qquad (5)$$

where $T_e = \epsilon_{e_2} - m_e c^2$ is the kinetic energy of the final electron. Here we have taken an average over the projection of the angular momentum of the initial electron, and we have summed over the final states of the neutrino and the electron.

The wave functions and energies of the atomic bound states are calculated by the relativistic self-consistent Hartree–Fock–Dirac method with a local exchange-correlation potential.[18] The partial radial wave functions of the outgoing electrons are found through a numerical solution of the Dirac equation. Here we use the same potential as for the wave functions of the discrete spectrum.

As targets we selected the atoms ^{19}F ($Z = 9$) and ^{96}Mo ($Z = 42$). One reason for choosing these atoms is that we can see the changes which occur in the influence of binding effects as we go from light atoms to intermediate-mass atoms. Another motivation is that fluorine is used in scintillation detectors in experiments which are being carried out today,[8] while atoms with Z's close to that of molybdenum can be used in calorimetric detectors which operate on the basis of a superconducting phase transition.[14]

Figure 1 shows calculated spectra of the recoil electrons knocked out of the K shell of the ^{19}F atom as the result of (a) the weak interaction and (b) the magnetic interaction. Here the energy of the impinging neutrino was $E_{\nu_1} = 100$ keV. Figure 2 shows the results of corresponding calculations for deep shells of the ^{96}Mo atom. Shown for comparison by the dashed lines are corresponding cross sections for scattering by the free electron:[11,19]

$$\frac{d\sigma^{(\omega)}}{dT_e} = \frac{G_F^2 m_e}{2\pi\hbar^4 c^2}\{(g'_V + g_A)^2 + (g'_V - g_A)^2(1 - T_e/E_{\nu_1})^2 + (g_A^2 - g_V'^2) m_e c^2 T_e / E_{\nu_1}^2\}, \qquad (6)$$

$$\frac{d\sigma^{(m)}}{dT_e} = \frac{\pi e^4 \mu_\nu^2}{m_e^2 c^4} \frac{1 - T_e/E_{\nu_1}}{T_e}. \qquad (7)$$

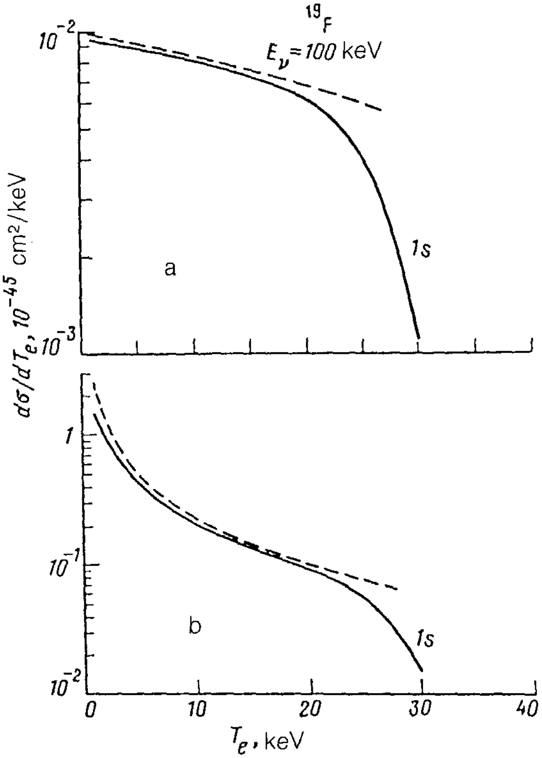

FIG. 1. a: Spectra of electrons knocked out of the K shell of the fluorine atom in the scattering of neutrinos with an energy $E_\nu = 100$ keV as a result of the weak interaction. b: The same, but as a result of the magnetic moment, $\mu_\nu = 10^{-10}\ \mu_B$. The dashed lines are spectra corresponding to free νe scattering.

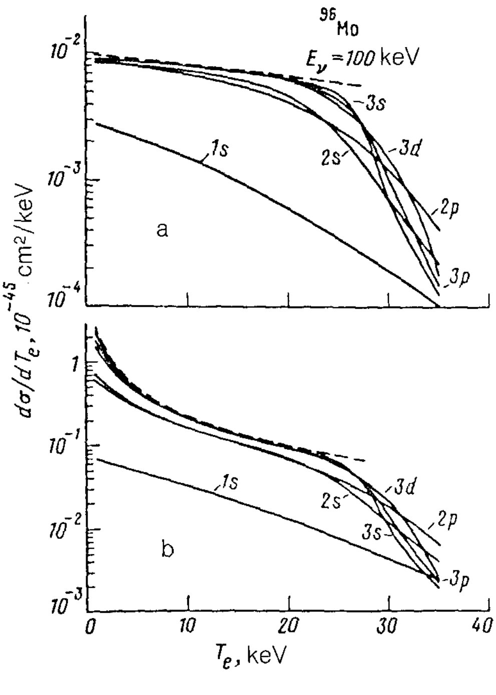

FIG. 2. Spectra of electrons knocked out of various shells of a molybdenum atom in the scattering of 100-keV neutrinos. The notation is the same as in Fig. 1.

TABLE I. Binding energies of subshells of the fluorine and molybdenum atoms (in eV).

Subshell	$1s_{1/2}$	$2s_{1/2}$	$2p_{1/2}$	$2p_{3/2}$	$3s_{1/2}$	$3p_{1/2}$	$3p_{3/2}$
F	662	31.7	13.6	13.5	–	–	–
Mo	19788	2798	2576	2470	479	394	377

Subshell	$3d_{3/2}$	$3d_{5/2}$	$4s_{1/2}$	$4p_{1/2}$	$4p_{3/2}$	$4d_{3/2}$	$5s_{1/2}$
F	–	–	–	–	–	–	–
Mo	227	223	67.9	43.7	41.2	6.8	6.1

The kinetic energy of the recoil electron in the last expression has the following upper bound, according to 4-momentum conservation:

$$T_e^{max} = \frac{2E_\nu^2}{2E_\nu + m_e c^2}. \tag{8}$$

Table I shows binding energies calculated for the electron subshells of these atoms, with the valence configuration $2p_{1/2}^2\ 2p_{3/2}^3$ in the case of fluorine and the configuration $4d_{3/2}^4\ 5s_{1/2}^2$ in the case of molybdenum.

All the curves in Figs. 1 and 2, as well as those in the following figures, correspond to cross sections per electron of the target atom. In all the calculations we assumed $\mu_\nu = 10^{-10}\mu_B$ and $\langle r^2 \rangle = 0$. The values of the constants were taken from Ref. 20.

At a neutrino energy $E_{\nu_1} = 100$ keV the spectra of electrons knocked out of the K shell of the fluorine atom are, on the whole, only slightly different from the free-scattering spectra. This was to be expected, since E_{ν_1} is more than two orders of magnitude greater than the binding energy of K electrons in this case. Even in this case, however, we see some significant differences in the spectra at $T_e \approx 20$ keV, near the upper kinematic limit in (8). These differences stem from momentum nonconservation in scattering by bound electrons. Such effects, which stretch out the hard part of the energy spectra of the recoil electrons (in contrast with the sharp cutoff in the case of free scattering), are characteristic of essentially all shells, as can be seen in Fig. 2. This figure shows the spectra of electrons which are knocked out of various shells of the molybdenum atom at the same neutrino energy, $E_{\nu_1} = 100$ keV. Here we see substantial overall differences from the free-scattering spectra, not only for the $1s$ (deepest) shell, whose binding energy in this case is smaller than the energy of the impinging neutrino, E_{ν_1}, by a factor of about 5, but also for the $2s$ and $2p$ shells, whose binding energies are smaller by an order of magnitude. The explanation for this result is that the differences in the cross sections are determined by the characteristic momentum nonconservation Δp_e in the scattering process. This quantity is equal in order of magnitude to the momentum of the electron in the shell under consideration $\Delta p_e \approx \alpha Z m_e c/n$, not to its binding energy $\epsilon_b \approx -(\alpha Z)^2 m_e c^2/2n^2$. On the T_e scale, this case corresponds to the interval $\Delta T_e \approx c^2 p_e \Delta p_e / E_e$ in which the cross sections $d\sigma/dT_e$ should indeed be different. At the upper edge of the recoil spectrum we find $\Delta T_e \approx 2(\alpha Z/n) E_\nu (1+x)/(1+2x+2x^2)$ using (8), where $x = E_\nu / m_e c^2$. In the

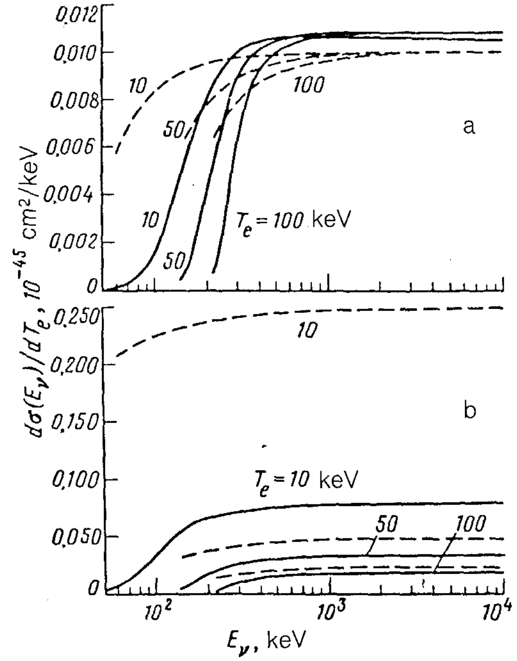

FIG. 3. Differential cross section for scattering by a K electron of the molybdenum atom versus the energy of the impinging neutrino, E_{ν_1}, for fixed kinetic energies of the recoil electron ($T_e = 10$, 50, and 100 keV; the curve labels). The notation is the same as in Fig. 1.

nonrelativistic case we have $\Delta T_e \approx 2\alpha Z E_\nu / n$. The results in Figs. 1 and 2 agree well with this estimate. At ultrarelativistic energies we have $\Delta T_e \approx \alpha Z m_e c^2 / n$. The relative contribution of the interval ΔT_e decreases in inverse proportion to E_ν.

It can be seen from Figs. 1 and 2 that the cross sections calculated for both weak scattering and magnetic scattering by bound electrons are smaller than those for free electrons, at all values of T_e. However, as E_{ν_1} increases, the situation regarding the weak scattering reverses, and the corresponding cross sections $d\sigma/dT_e$ for atoms become larger than the free-scattering cross sections. This effect is demonstrated in Fig. 3, which shows differential cross sections $d\sigma/dT_e$ for electrons knocked out of the molybdenum K shell at fixed recoil energies $T_e = 10$, 50, and 100 keV. These cross sections are plotted against E_{ν_1} over the broad range up to $E_{\nu_1} = 10$ MeV. We see that at small values of E_{ν_1} the "weak" K-electron cross section is smaller than the free-electron cross section. As E_{ν_1} increases, this weak cross section becomes $\approx$5–10% larger and then asymptotically approaches the free cross section from above.

For the magnetic scattering, the cross sections for the bound electrons are smaller than those for free electrons everywhere. The most important effect in this case is the appearance of a natural cutoff of the divergence of recoil spectrum (7) at small values of T_e in the case of scattering by free electrons. The reason for this effect is simple: When we go from free electrons to bound electrons, with a binding energy ϵ_b, we must make the substitution $T_e \to T_e + \epsilon_b$ in (7) as $T_e \to 0$. We would expect that the ratio of the two cross sections would be determined at $E_{\nu_1} \gg T_e$ by the factor $(T_e + \epsilon_b)/T_e$ and that the electron spectrum would reach a plateau as $T_e \to 0$. The calculated results shown in Fig. 4b confirm this expectation.

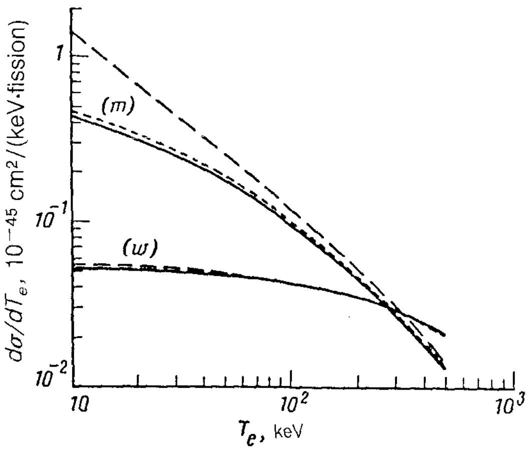

FIG. 4. Spectra of electrons knocked out of the K shell of the molybdenum atom by reactor $\tilde{\nu}_e$'s as a result of the weak interaction (ω) and the magnetic interaction (m). These calculations were carried out with $\mu_{\tilde{\nu}} = 10^{-10}\,\mu_B$ and the $\tilde{\nu}_e$ spectrum from the fission fragments of ^{235}U (Ref. 11). The long-dash lines correspond to free scattering, and the solid lines to an exact calculation. The short-dash line was found by multiplying the spectrum for free magnetic scattering by a factor $T_e/(T_e+\epsilon_b)$, where ϵ_b is the binding energy of the K electrons in ^{96}Mo.

What effects might atomic binding have in the scattering of electron antineutrinos $\tilde{\nu}_e$ from a fission reactor? From the experimental standpoint, a fission reactor is the most appropriate source for studying νe scattering. The typical reactor of a nuclear power plant emits $\approx 5\times 10^{20}$ $\tilde{\nu}_e$'s per second. Their energies are comparatively low: The energy spectrum of reactor $\tilde{\nu}_e$'s ranges up to about 10 MeV, peaking at $E_{\tilde{\nu}_e} < 1$ MeV. What is to be measured is the spectrum of recoil electrons, which is given by the expression

$$\overline{\frac{d\sigma}{dT_e}} = \int_{E_{\tilde{\nu}_e}^{\min}(T_e)}^{\infty} n(E_{\tilde{\nu}_e})\frac{d\sigma(E_{\tilde{\nu}_e})}{dT_e}dE_{\tilde{\nu}_e}, \tag{9}$$

where $n(E_{\tilde{\nu}_e})$ is the spectrum of reactor $\tilde{\nu}_e$'s, and the integration over $E_{\tilde{\nu}_e}$ is carried out from a lower limit $E_{\nu_e}^{\min}$. For free scattering, this lower limit is found from (8) at a fixed kinetic energy T_e; for scattering by a bound electron, it is instead found from energy conservation ($E_{\tilde{\nu}_e}^{\min} = T_e + \epsilon_b$). Using the spectrum of reactor $\tilde{\nu}_e$'s from ^{235}U fission fragments,[11] we calculated the differential cross sections in (9) for electrons knocked out of the K shell of the ^{96}Mo atom. Figure 4 shows the results for the interval $10 \leqslant T_e \leqslant 500$ keV. We see that atomic-binding effects are negligible in weak scattering. In magnetic scattering, in contrast, these effects are extremely noticeable, particularly at low values of T_e. It is a good approximation to deal with these effects by simply multiplying the cross section for free magnetic scattering by a factor $T_e/(T_e+\epsilon_b)$, as can be seen by comparing the short-dash line in Fig. 4 with the corresponding exact calculation. At $T_e = 10$ keV, the difference between the approximate calculation and the exact calculation is $\approx 7.5\%$, while at $T_e = 500$ keV it is $\approx 4\%$.

The effects which we have been discussing here may be important for planning experiments on νe scattering and in analyzing the data, particularly if atoms of intermediate-mass or heavy elements are used as targets.

We wish to thank E. Kh. Akhmedov and S. V. Tolokonnikov for useful discussions and A. A. Soldatov for furnishing the program for calculating the electronic structure of an atom. One of us (S.F.) is extremely indebted to F. von Feilitzsch for hospitality during a visit to the Technical University of Munich in May of 1991, when this study was begun, and also for some stimulating discussions.

[1]R. Davis, Jr., *Talk at the Twenty-First International Conference on Cosmic-Ray Physics*, Adelaide, Australia, 1990.
[2]K. Lande, *Talk at Neutrino-90: Fourteenth International Conference on Neutrino Physics and Astrophysics*, CERN, Geneva, June 1990.
[3]L. Wolfenstein, Phys. Rev. D **17**, 2369 (1978).
[4]S. P. Mikheev and A. Yu. Smirnov, Yad. Fiz. **42**, 1441 (1985) [Sov. J. Nucl. Phys. **42**, 913 (1985)].
[5]M. B. Voloshin, M. I. Vysotskiĭ, and L. B. Okun', Zh. Eksp. Teor. Fiz. **91**, 754 (1986) [Sov. Phys. JETP **64**, 446 (1986)].
[6]E. Kh. Akhmedov, Phys. Lett. B **257**, 163 (1991).
[7]F. Reines, H. S. Gurr, and H. W. Sobel, Phys. Rev. Lett. **37**, 315 (1976).
[8]G. S. Vidyakin *et al.*, Mosc. Phys. Soc. **1**, 85 (1991).
[9]S. V. Tolokonnikov and S. A. Fayans, Izv. Akad. Nauk SSSR, Ser. Fiz. **37**, 2667 (1973).
[10]A. V. Kyuldjiev, Nucl. Phys. B **243**, 387 (1984).
[11]P. Vogel and J. Engel, Phys. Rev. D **39**, 3378 (1989).
[12]R. C. Allen *et al.*, Phys. Rev. Lett. **55**, 2401 (1985); **64**, 1330 (1990).
[13]G. G. Raffelt, Phys. Rev. Lett. **64**, 2856 (1990).
[14]F. von Feilitzsch, in *Test of Fundamental Laws in Physics* (ed. Fackler and Trân Tranh Vân) (Editions Frontières), Ninth Moriond Workshop, 1989, pp. 435–441.
[15]H. Bethe, Proc. Cambr. Phil. Society **35**, 108 (1935).
[16]G. V. Domogatskiĭ and D. K. Nadezhin, Yad. Fiz. **12**, 1233 (1970) [Sov. J. Nucl. Phys. **12**, 678 (1971)].
[17]S. L. Glashow, Nucl. Phys. **22**, 579 (1961); S. Weinberg, Phys. Rev. Lett. **19**, 1264 (1967); A. Salam, in *Elementary Particle Theory* (ed. N. Svatholm), Almqvist and Wiksell, Stockholm, 1968, p. 367.
[18]V. L. Moruzzi *et al.*, *Calculated Electronic Properties of Metals*, Pergamon, New York, 1978.
[19]G. 't Hooft, Phys. Lett. **37**, 195 (1971).
[20]Particle Data Group, Phys. Lett. **239**, 1 (1990).

Translated by D. Parsons